

A New Antispoofing Approach for Biometric Devices

P. Venkata Reddy, Ajay Kumar[†], S. M. K. Rahman, Tanvir Singh Mundra

Abstract— The deployment of fingerprint sensors is increasingly becoming common and has now gained high user acceptance. However, fingerprint sensors are susceptible to spoofing using artificial materials or in worst case to the dismembered fingers. Fake/gummy fingerprints have shown to fool most commercial fingerprint systems. This paper proposes a new method of anti-spoofing using reliable liveness detection. The proposed method of liveness detection is based on the principle of pulse oximetry and involves the source of light originating from a probe at two wavelengths. The light is partly absorbed by haemoglobin, by amounts which differ depending on whether it is saturated with oxygen or deoxygenated haemoglobin. We then perform the computations for the absorption at two wavelengths to estimate the proportion of haemoglobin which is oxygenated. The computed percentage of oxygen in the blood, along with the heart pulse rate, determines the liveness of the enrolled biometric. Our experimental results demonstrate that the developed prototype can successfully thwart the spoof attacks (including those based on dismembered fingers).

Index Terms— Antispoofing, biometrics, fingerprint antispoofing, liveness detection, pulse oximetry.

I. INTRODUCTION

Recent research and tests have show that with negligible-to-modest effort, many leading biometric technologies are susceptible to attacks in which fake fingerprints, static facial images, static iris images can be used successfully as biometric samples. These fraudulent samples are processed by the biometric system to generate templates and to verify enrolled individuals. Methods of attack include fashioning fingerprints from gelatin, superimposing iris images atop human eyes, and even breathing on a fingerprint sensor. All biometrics are vulnerable to spoofing from the smartly faked copies.

- Hand Geometry and Palm print acquisition devices can be easily spoofed.
- Biometric samples are vulnerable to spoof attacks and should no longer be considered a secret.
- The survival of biometric identification technologies will depends on its ability to reject fake samples.

The answer to the above problems lies in *Liveness Detection Countermeasures*. In general, a biometric system may have to cope up spoof attacks at two levels; sensor level and data level. The data level attacks involve spurious transmission of the sensed data, template data or matching score data at key intersections to achieve the favorable decision [32]. The imposter attacks at data level are not considered in this work. The objective of our work is to introduce a new capability in the biometric system to detect during enrollment and identification or verification, whether the biometric sample presented is alive or not. Furthermore, since our system is designed to protect against the attacks from artificial fingerprints, it must also

check that the presented biometric sample belongs to the live human being who was originally enrolled in the system and not just any live human being. Many users believe that the current biometric systems can detect liveness in the presented biometric. Some manufacturers of biometric system also claim to have liveness detection in their system. It has however been shown that fingerprint systems can be fooled with artificial fingerprints, that static facial images can be used to fool face recognition systems [23], and that static iris images can be used to fool iris recognition systems [5].

A. Prior Work and Motivation

The fingerprint of a person enrolled in a database is easy to acquire, even without the user's knowledge and cooperation. The latent fingerprint impressions on the daily-use products or on sensors of access control may itself be lifted and used as templates [4]. Successful experiments in creating fake fingers and spoofing commercially available fingerprint sensors have been reported by Putte and Keuning [8] and by Matsumoto *et al.* [25]. Schuckers [13] has presented a detailed study on the detection of liveness and fake biometric samples for the fingerprint based systems. Uludag and Jain [14] use hill climbing approach to synthesize target feature templates that can guarantee positive identification in small number of attempts. Moon *et al.* [22] have analyzed surface coarseness of high resolution fingerprint images and proposed wavelet based approach for liveness detection. Another texture analysis based liveness detection test for fingerprint images is reported in [25]. Recently, Antonelli *et al.* [21] have proposed the detection of fake fingers from the video analysis of distortion pattern generated on the surface.

Researchers have suggested several *liveness* countermeasures to avoid *sensor level* spoof attacks: finger response to electrical impulse [17], finger temperature and electrocardiographic signals [15], and time varying perspiration patterns from fingertips [3]. Despite variety of these suggestions only few have been implemented [24] and there has been no investigation to ascertain the effectiveness of these approaches in liveness detection for fingerprint devices.

The measurement of the percentage of oxygen in the blood has been known in the literature [26]-[27] and used in the medical measurements. However, there has not been any systematic study to illustrate its usefulness/effectiveness as an antispoofing technique for the fingerprint identification. Therefore the objective of our work was to design, develop and investigate the utility of oxygenated blood measurements for fingerprint antispoofing. We propose a low-cost, fully automated design that works simultaneously with fingerprint identification device and reliably thwarts sensor level spoof attempts. The developed system combines pulse oximetry with the fingerprint sensing and can be easily integrated to any existing fingerprint devices.

[†] Corresponding Author, Email: ajaykr@ieee.org

B. Proposed System

The block diagram of the proposed anti-spoofing system using online liveness detection is shown in figure 1. The estimation of percentage of the oxygen saturated blood, in the presented finger, relies on the extraction and measurements from the transmitted signals. The most important part of the system is the pulse oximeter sensor, which interacts with the finger while its being imaged for identification and has two LEDs for emitting different wavelengths of light, *i.e.* red (660 nm) and near infrared (940 nm).

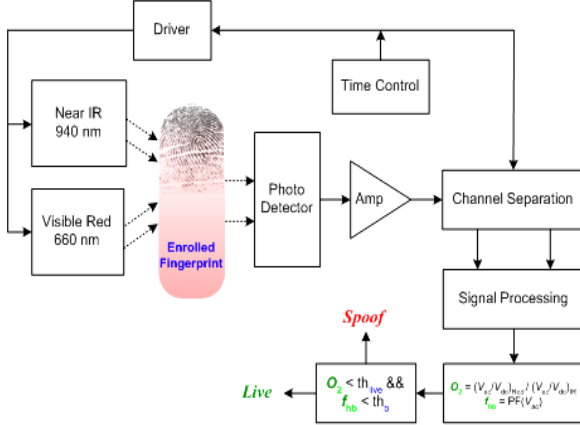


Figure 1: Block diagram of proposed anti-spoofing system

The pulses generated by the timing and control circuit are given to the driver circuit, which drives the two sources of light. These sources are excited alternatively at high speed. The matched photo detector detects the reflected light and the corresponding photo current is converted into voltage by current to voltage converter. The voltage signal corresponding to each of the received light frequencies is separated by channel separation mechanism, which synchronizes the sampling of signals with the excitation of corresponding emitters. The separated signals are filtered to remove noise and unwanted high frequency components and are further processed to get the *AC* and *DC* components in each signal. These components are used to estimate R , which we refer as *Liveness Factor* in this paper. The *Liveness Factor* is essentially the representation of the proportion of oxygen saturated blood ($SpO_2\%$) and is detailed in the following section. The magnitude of R is compared with the threshold to decide the liveness of the introduced biometric sample.

II. LIVENESS DETECTION

The liveness detection method proposed and implemented in this paper is based on pulse oximetry, in which the saturation of oxygen of haemoglobin is measured; heart pulse from the tip of the finger is detected; and used as liveness detection measure. The absorption of visible light by a haemoglobin solution varies with oxygenation. This is because the two common forms of the molecule, oxidized haemoglobin (HbO_2) and reduced haemoglobin (Hb) have significantly different optical spectra in the wavelength range from 500 nm to 1000 nm [2]. The oxygen chemically combined with haemoglobin inside the

red blood cells makes up nearly all of the oxygen present in the blood. The oxygen saturation SpO_2 is defined as the ratio of oxyhaemoglobin (HbO_2) to the total concentration of haemoglobin present in the blood.

$$SpO_2 = \frac{HbO_2}{[Hb + HbO_2]} \quad (1)$$

The arterial SpO_2 is a parameter measured with oximetry and is normally expressed as a percentage. The difference in the absorption spectra of HbO_2 and Hb can be utilized for the measurement of arterial oxygen saturation in vivo. The wavelength range between 600 nm and 1000 nm is also the range for which the attenuation offered by the body tissues is minimal. If we assume that the transmission of light is only influenced by the relative concentrations of HbO_2 and Hb , and their absorption coefficients at the two measurement wavelengths, then the intensity of light transmitted through the arterial blood decreases logarithmically with path length, as illustrated by the Beer-Lambert law [6]. If the artery is of length l_a through which light, initially of intensity $I_{in}(t)$ is passed, then this law suggests that:

$$\begin{aligned} I_1(t) &= I_{1in}(t) * 10^{-(\alpha_{o1}C_o + \alpha_{r1}C_r)l_a} \\ I_2(t) &= I_{2in}(t) * 10^{-(\alpha_{o2}C_o + \alpha_{r2}C_r)l_a} \end{aligned} \quad (2)$$

where, C_o is the concentration of oxyhaemoglobin (HbO_2), C_r is the concentration of reduced haemoglobin (Hb), α_{on} is the absorption coefficient of HbO_2 and α_{rn} is the absorption coefficient of Hb at wavelength λ_n . The $I_1(t)$ and $I_2(t)$ represent the intensity of light at wavelengths λ_1 and λ_2 respectively.

With the light at 660 nm, deoxygenated haemoglobin has a higher absorption, whereas at 940 nm, oxygenated haemoglobin has a higher absorption. Once the absorption levels are detected, it is possible to determine the ratio of the absorption between the deoxygenated and oxygenated haemoglobin at the different wavelengths. The photons from the emitter pass through the skin. Although, some scattered light escapes through the finger, it will be assumed that the light emitted is absorbed solely by the anatomy of the finger and the photo detector [5].

$$I(t) = I_0(t)e^{-\epsilon(\lambda)cd} \quad (3)$$

where, $I_0(t)$ is the original intensity of the light, $\epsilon(\lambda)$ is the extinction coefficient of absorbability at a specific wavelength λ , c is the concentration of the substance absorbing the light, and d is the optical path length. The pulsatile flow of arterial blood occurs at the cardiac cycle systole phase and the light absorption varies proportionately to the flow of blood. This varying component due to absorption of light through tissue is called the pulsatile component and it is the *AC* component and represents the difference in absorption of light by oxygenated and deoxygenated haemoglobin of the arterial blood. The *DC* component in the reflected signal is affected primarily by the absorption of light due to tissue bed, venous blood, non pulsatile arterial blood and the intensity of the light from the incident source, ambient light. The number of beats per minute is also calculated, yielding the pulse rate.

III. DESIGN AND IMPLEMENTATION

The initial design of the proposed prototype device for liveness detection employed analog approach. However, with analog components the response of the device was very sluggish, due to the slow charging of the capacitors at the low pass filter stages, and the complexity of the device was high to extract a low amplitude biomedical signal in the presence of noise. In order to account the phase shift between the red and infra-red signals peak detectors were employed. This resulted in slow response time of the system as the capacitors charged to their peak value had to comeback to a lower voltage level. In order to speed up the response and to facilitate the integration with a fingerprint sensor, the final implementation (figure 2) was initiated using a microcontroller that had most of the instructions implemented as single cycle instructions.

Several fingerprint devices are standalone USB devices so the microcontroller (MCU) with this type of interface was preferred for easy integration. The AVR microcontroller AT90USB1287 [10] was found suitable for implementation as it is having an USB and RS232 interface, along with sufficient programmable Flash memory (128K) and on-chip EEPROM (8K) for complete data acquisition and processing. An on-chip bootloader permits very quick firmware download from a PC, without using a parallel programmer or dedicated hardware. In

System Programming (ISP) of the chip entails to update the software using simple two wire serial interface to connect to a PC, without the need to remove the controller or use some dedicated programming hardware.

A. Signal Acquisition

We implemented the entire steps of signal processing for the acquired signals in digital domain to effectively and quickly filter the associated noise. The fast Pulse Width Modulation (PWM) mode of AT90USB1287 [10] provides a high frequency PWM waveform generation option. The PWM channel 1 with the Timer1 is programmed by loading the Output Compare Registers (OCR1A and OCR1B) to generate a PWM pulses with ON time of 500 μ s and OFF time of 7500 μ s, the clock count is started with the time period of 7500 μ s.

Emitter of the sensor gets the excitation signal from the PWM output at I/O port pins PB6 and PB4 of AT90USB1287 (figure

2). In order to increase the intensity of light that the emitter of the pulse oximeter sensor can emit, an increased amount of current is passed through the sensor for a short duration of time (ON time) with the help of driving transistor. The timer pulses (figure 3) are given to the base of the driving transistor through a series capacitor, which acts as a high pass filter, to protect the sensor emitter from being spoilt by controller hang-up.

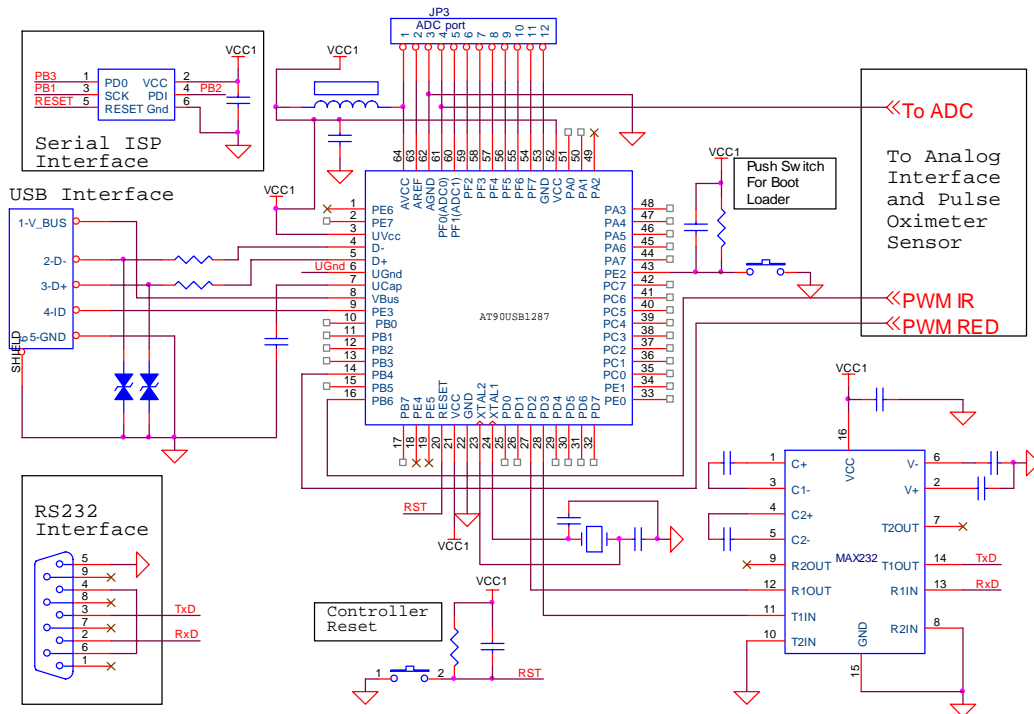


Figure 2: Microcontroller integration with serial and sensor interface

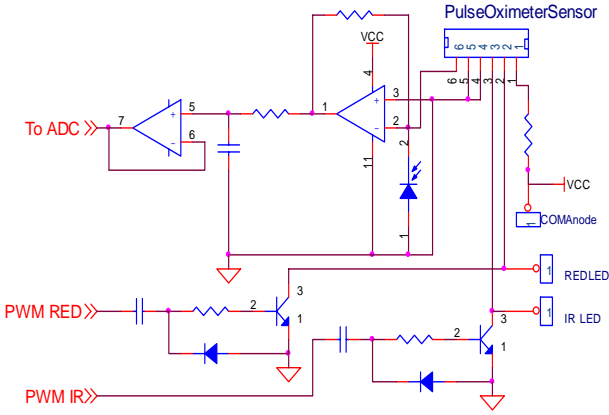


Figure 3: Implementation of PWM and signal acquisition

The matched photo detector detects the light in the range 300-1100 nm and it has its peak response at 660 nm and 940 nm. The signal from the matched photo detector corresponding to red (660 nm) wavelength light has to be separated from the infra-red (940 nm) wavelength light without interference. This is achieved by synchronization between the emitter excitation and the acquiring of received signal at the output of photo detector. The time duration between the 660 nm pulse and the 940 nm excitation pulse is 500 μ s with 660 nm pulse followed by 940 nm. The photo current is converted into voltage by a current to voltage converter. This voltage signal comprises of high frequency components, *i.e.*, signals due to noise induced by ambient light. The high frequency noise is removed by low pass filtering with a cutoff frequency of 1.59 kHz. The signal after low pass filtering is given to one of the ADC channels with a buffer in between to decrease the effects of loading the output signal by ADC of the controller. The on-chip ADC is a successive approximation analog to digital converter, with a reference voltage of 2.56 V and a conversion time of 70 μ s.

B. Finger Presence Detection

The detected signal from the photo detector is measured after every 8 m sec and the sampled ADC value is compared with the fixed threshold value of 0x1FF (1.28V). If the signal acquired is below the threshold voltage level, the finger is present and the status is marked as PRESENT, the periodic sampling of signal by ADC starts and at the same time fingerprint sensor is enabled.

C. Synchronization of Red and IR Signal Acquisition

The Red and IR signals are acquired by the controller at the ADC channels by starting conversion only at the occurrences of the corresponding PWM pulse. This ensures that the detector detects the transmitted light from the fingerprint sample only at the Red and IR excitation pulses at the emitter, and is in synchronization with the transmitted signal. This makes it almost impossible for the attacker to pulse and synchronize a pair of infra-red and red LEDs underneath the gummy fingerprint and successfully spoof the system.

D. Ambient Light Removal

The detector output sample is taken just before every PWM pulse (red and IR) and digital signal level is subtracted from the very next digital values of the analog signal measurements taken at pulse intervals when the emitter is excited.

E. D/A conversion using PWM

The TIMER0 of the microcontroller is configured to change the time interval of the generated PWM pulses, which corresponds to the analog values read at the ADC input. When this PWM pulse output is passed through low pass filter we get the analog equivalent of the original signal being acquired.

F. Filtering

The filtering is required to eliminate high frequency noisy components and extract low frequency signal of our interest. In our implementation, a low pass digital filter which makes the averaging of 10 neighborhood samples was employed.

$$z(n) = \sum_{k=0}^{9} x(k)h(n-k) \quad (4)$$

where $z(n)$ is the filtered sequence, $x(k)$ is the input sequence, and $h(n)$ is the impulse response of the low pass filter. The samples from the acquired signal are also reproduced in figure 7. The convolution of the red and infrared sample sequence, with the filter sequence, generates corresponding moving average filtered sequences in which the high frequency noisy components are attenuated.

IV. LIVENESS ESTIMATION AND INTEGRATION

A. AC-DC components Extraction

The measurements on the detected and processed signals are used to ascertain the percentage of oxygen saturated blood. The magnitude of AC and DC component measurement in the filtered samples, for red (660 nm) and infrared (940 nm), requires measuring the minimum and maximum values of the corresponding sample sequences. The difference of minimum and maximum is calculated and this is the peak to peak amplitude of each sequence. The average of the minimum values of the samples in each case is calculated for both the sequences which represent the absorption of light due to tissue, fat and non pulsatile part of the haemoglobin.

The peak-to-peak amplitudes (V_{pp}) correspond to the AC component of the signals and some part of the DC components. These are calculated as follows:

$$V_{dc} = V_{min} + V_{pp} / \pi \text{ and } V_{ac} = V_{pp} / \sqrt{2} \quad (5)$$

where, V_{ac} and V_{dc} represent the measured AC and DC components of the samples.

B. Calculation of R

The estimation of the oxygen saturated blood, *i.e.* SpO₂%, uses classical approach under assumption of a homogenous Beer-Lambert transmission model cited in section II. The two equations in (2) are solved to compute SpO₂ [29]:

$$SpO_2 = \frac{1}{1 - \frac{kR\varepsilon_o(\lambda_1) - \varepsilon_o(\lambda_2)}{kR\varepsilon_d(\lambda_1) - \varepsilon_d(\lambda_2)}} \quad (6)$$

where, $\varepsilon_o(\lambda_1)$ and $\varepsilon_o(\lambda_2)$ are the extinction coefficient of absorbability for oxygenated hemoglobin at wavelengths λ_1 and λ_2 respectively, while $\varepsilon_d(\lambda_1)$ and $\varepsilon_d(\lambda_2)$ are the corresponding extinction coefficients for the deoxygenated hemoglobin. Note that even though equation (6) is the required solution for SpO_2 , both k and R are functions of unknown optical properties of the tissue. The quantity R is the ratio of the logarithmic derivatives of the received intensities, or equivalently the ratio of the normalized derivatives;

$$R = \frac{\Delta \ln I_1(t)}{\Delta \ln I_2(t)} = \frac{I_2(t)\Delta I_1(t)}{I_1(t)\Delta I_2(t)} \quad (7)$$

In order to determine the *Liveness Factor R*, from the pulsatile light intensities to non-pulsatile light intensities, the constant DC component of the light intensity must be factored out. The amplitudes of both the AC and DC components are dependent on the incident light intensity. Dividing the AC level by the DC level gives a 'corrected' AC level that is no longer a function of the incident light intensity. The ratio of the AC and DC components for the red (660nm) and infra-red (940nm) is measured with the following equation.

$$R = \frac{(AC_{660} / DC_{660})}{(AC_{940} / DC_{940})} = \frac{(V_{AC} / V_{DC})_r}{(V_{AC} / V_{DC})_{ir}} \quad (8)$$

V_{AC} and V_{DC} are the correspondingly AC and DC components for red (660 nm) and infra-red (940 nm) samples. In a nonturbid medium, $k = 1$, which is the reasonable approximation employed in pulse oximetry [29]. Thus the *Liveness Factor R* itself represents the saturated oxygen ($SpO_2\%$) in haemoglobin. An empirically derived calibration curve [1] for the relationship between R and $SpO_2\%$ provides the pulse oximetry oxygen saturation level $SpO_2\%$. This calibration curve is employed to build a lookup table (LUT) illustrated in table 1. The $SpO_2\%$ values for $R > 2.8$ (corresponding to $SpO_2\% < 30\%$) are considered non-live and are forced to zero. If the oxygen saturation level $SpO_2\%$ is above 30% the introduced biometric is designated as live otherwise it's treated as non-live.

Table 1: Look up Table for R and $SpO_2\%$

R	0.4	0.6	0.8	1.0	1.2	1.4	1.6	1.8
$SpO_2\%$	100	96	90	85	80	75	68	62
R	2.0	2.2	2.4	2.6	2.8	3.0	3.2	3.4
$SpO_2\%$	56	50	43	37	31	24	16	8

C. Liveness Integration by Negotiation

The decision on liveness of the introduced sample by the liveness detection device (host controller) determines whether the negotiation has to be done or not. If the host controller decision is live then the fingerprint identification decision is activated and for non-live decision the integration of the fingerprint decisions from simultaneously captured fingerprint images is suspended. In the process of integration of the fingerprint sensor the host controller communicates with the

fingerprint device through full-duplex serial communication protocol and performs the operation specified by command byte value in the command field of the packet sent by host controller. The flow chart shown in figure 4 summarizes the operation and the implementation of our approach.

D. Communication with Fingerprint Device

The fingerprint sensor is powered up by the power source of 5V which comes either from the USB bus power or external power supply. One of the RS232 channel is connected to the serial interface of the host controller (liveness detection device). The RS-232C communication setup is with a baud rate 9600 bps (1 start-bit, 8 data-bits, 1 stop-bit and no parity bit). The embedded fingerprint device employed to generate fingerprint matching decision uses ARM7 processor. Figure 5 shows snapshot of the liveness detection device developed for our investigation. The fingerprint device performs an action given by the command in the command field of the packet sent by the host controller. Each acknowledgement packet is compared with the predefined packets to determine the response from the fingerprint sensor. If the host controller gets the Identification Success, or Failure, or Capture Timed out from the fingerprint device then it determines whether the user is to be accepted or rejected.

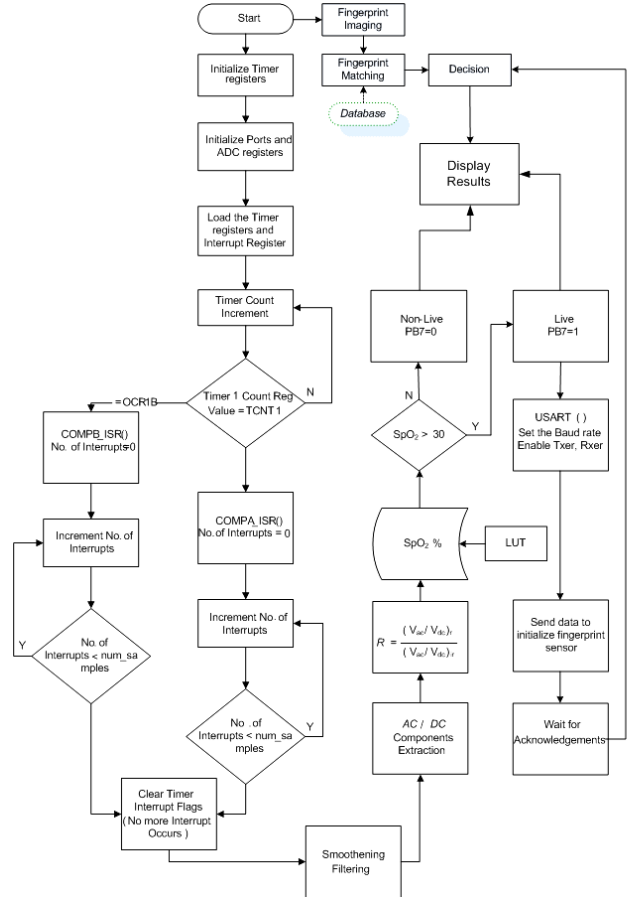


Figure 4: Operation of automated liveness detection and its integration with fingerprint device

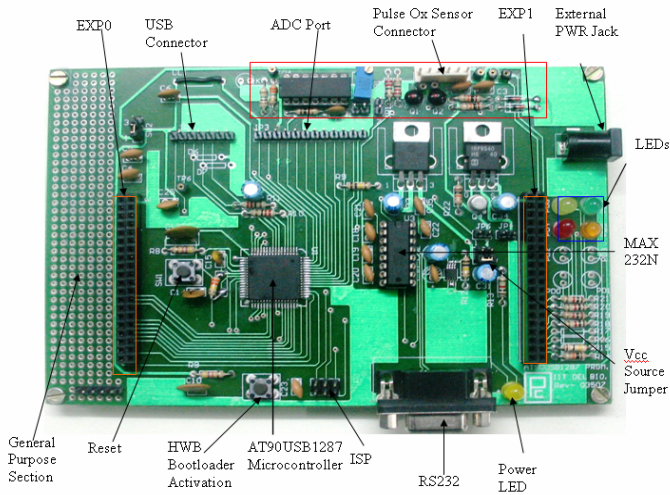


Figure 5: Development of interfacing board

V. EXPERIMENTS AND RESULTS

The implementation of the proposed liveness detection module was carried out as detailed in section III and IV. This device was integrated with an embedded fingerprint matcher as discussed in previous section. The rigorous testing results from the implemented system have illustrated the success of the device in detecting spoof attempts. Some of the experimental results and observations from the developed system are reproduced.

In order to ascertain the performance of the developed liveness detection module, we investigated its performance on spoof attacks using artificial fingers. The spoof fingers are made using M-seal to firstly construct the fingerprint molds. Then the artificial fingerprint is obtained from these molds using the gelatin powder (using equipments from Bio Research Organic Laboratory, at IIT Delhi, for conditioning the surface). In addition to the preparation of just thin layers reproducing the fingerprints, we also made whole 3D fake fingers. These gummy fingers were made with Play-doh as in shown in figure 6.



Figure 6: Mold, Play-doh artificial finger and artificial fingerprint.

The acquired signal samples for an interval of 1.6 seconds for the live and non-live fingerprint samples are shown in the figure 7. These samples are having superimposed noise which causes small variation in the envelope of the signal and was taken care by applying sliding window averaging filter with 10 samples to smooth the acquired signal. Figure 7 also shows the

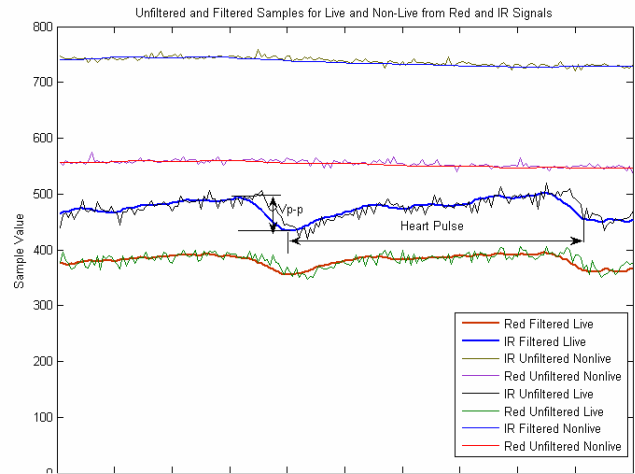


Figure 7: Unfiltered and filtered samples from red and infra-red signal using live and non-live samples

corresponding filtered signals which generate reliable measure of the *AC* and *DC* components. In the case of a live sample, the presence of heart pulse along with the change in amplitude with the IR and Red signals results in variation of the signal. But in the case of non-live fingers the pulsating nature of the signal is absent and the variation in the samples is very small. The *AC* values for the non-live case are not varying even with slight change in the position of its placement.

Table 2 shows the Red and IR signal measurements along with their corresponding *R* and $SpO_2\%$ values from the seven artificial fingers that simulate the spoof attacks. In order to ascertain the variation in signal measurements from the real live fingers, we gathered data from 18 volunteers (males and females between 17 to 58 years of age) using the developed device. The experimental results in table 3 suggest the regular variation in the *AC* and *DC* components among different persons from the live fingerprints. However, the relative change between IR and Red is quite small among different live fingerprints and therefore a threshold of 30% is judicious.

The *Liveness Factor R* calculated using equation (8) from the Non-live samples is very high, *i.e.* more than 6, and it doesn't come within the range of *R* values measured from the live samples. The *AC* and *DC* component measured from the live samples are highly separated from the corresponding measurements using non-live samples, especially with IR light as it is color independent and varies very little. This is despite the fact that the reflected light from red light is color dependent on the sample and changes the factor *R* calculated by equation (8). The estimated *R*, as expected, is in the non-live range from the spoof fingerprint samples and well separated (far below) from the threshold, which is empirically selected as 2.8 for *R* values. The corresponding $SpO_2\%$ for the decision threshold is 30% as shown in figure 8.

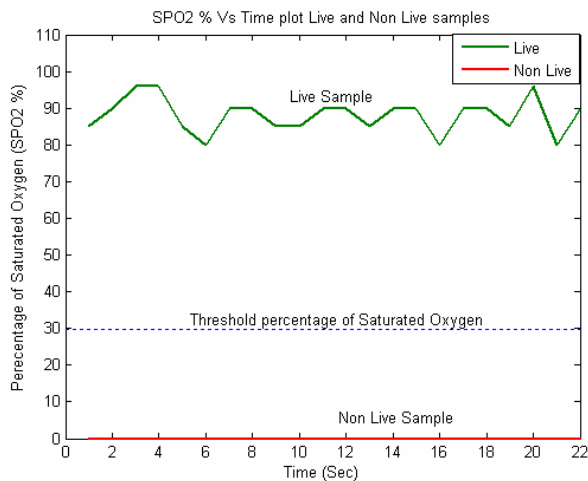


Figure 8: Live Vs Non-live estimation of SpO₂% values in an interval of 22 seconds

VI. DISCUSSION

The selection of threshold for the estimated SpO₂% is quite critical for the success of this approach. The SpO₂% threshold can significantly vary in the live persons with their individual medical conditions; e.g. carboxyhemoglobin, anemia, hypovolemia/hypotension, hypothermia, etc [33]. Furthermore the SpO₂% for the individuals can drastically change (up to 15%) if more than one of the above conditions hold simultaneously. In general, the theoretical value of SpO₂% for a conscious person can go up to 70%. In addition, the operating environmental conditions also have a profound effect on the measured SpO₂ values. The accurate measurement of the ambient light and its complete removal from the received signal is extremely difficult. The system could be kept in a completely dark room with no ambient light or be installed outdoor under the sun, where the contribution of the ambient light is quite substantial. Under these varied

Table 2: The AC and DC components, R value and SpO₂% for Non-Live

S. No.	Red AC value	Red DC Value	IR AC Value	IR DC Value	Red Minimum AC Value	Red Minimum DC Value	IR Minimum AC Value	IR Minimum DC Value	Ratio R	SpO ₂ %
1	7	51	6	446	5	50	6	440	10.2026	0
2	8	75	5	755	3	75	5	753	16.1067	0
3	35	317	1	1012	34	317	3	1011	111.7350	0
4	3	10	6	823	3	9	5	820	41.1530	0
5	18	145	7	979	17	141	5	972	17.3616	0
6	19	143	5	233	17	143	5	232	6.1916	0
7	24	187	4	695	10	183	4	687	22.2995	0
Average	16.286	132.571	4.857	706.143	12.714	131.143	4.714	702.143	32.1500	0

Table 3: The AC and DC components, R value and SpO₂% obtained for Live

S. No.	Red AC value	Red DC Value	IR AC Value	IR DC Value	Red Minimum AC Value	Red Minimum DC Value	IR Minimum AC Value	IR Minimum DC Value	Ratio R	SpO ₂ %
1	19	128	52	363	15	122	45	352	1.036208	85
2	43	285	70	367	40	278	66	350	0.791028	90
3	26	251	90	566	25	200	78	310	0.651439	90
4	25	170	60	476	22	165	51	454	1.166667	85
5	32	244	40	457	23	237	33	457	1.498361	80
6	26	176	47	305	22	151	45	276	0.958656	90
7	19	98	33	194	17	96	33	190	1.139765	85
8	18	113	51	382	17	110	40	390	1.193129	85
9	24	136	41	269	22	130	28	248	1.157819	85
10	47	359	84	664	45	333	80	568	1.034885	85
11	44	248	95	485	28	196	44	325	0.905772	90
12	26	191	95	619	20	153	42	402	0.886966	90
13	36	284	65	587	30	276	64	545	1.144745	85
14	22	166	70	449	21	164	67	465	0.850086	90
15	27	315	42	424	20	327	38	442	0.865306	90
16	21	115	41	351	16	113	30	298	1.563309	75
17	29	143	54	216	17	134	37	219	0.811189	90
18	24	134	34	264	18	107	30	194	1.390694	80
Average	28.222	197.556	59.111	413.222	23.222	182.889	47.278	360.278	1.05811	86.111

operating conditions, the 100% linearity and high accuracy of the sensors cannot be assumed. Secondly, the movement/placement of the finger during the sampling process and varying magnitude of pressure applied while enrolling the sample induces inaccuracy in the reflected signal and the corresponding SpO₂ value. Under strictly controlled environments this effect may be reduced, but it is not prudent to make such assumptions in general for practical purposes. Thirdly, the skin pigmentation and body fat also introduce errors in the SpO₂ values measured due to varied absorption coefficients [31]. Due to the physical constraints beyond our control, our system cannot be used on the finger tips or ear lobes where the readings are relatively more accurate.

In summary, a high value of SpO₂% threshold cannot account for significantly varying individual medical conditions and environmental conditions. Therefore the high value of the threshold will increase the false rejection rate (FRR) of this antispoofing system. On the other hand, if the SpO₂% threshold is kept low, the spoof attempts have more chances of acceptance and thereby increasing the false acceptance rate (FAR) of this system.

The liveness detection from fingerprints can also be ensured by acquiring the pulse, from the tip of fingers, which are generated from the autonomic nervous system. However, the problem with this approach is that it requires users to hold his/her fingers up to four seconds. Also, the pulse can be transmitted from a live finger on which a thin spoofing material is worn. On the other hand, the approach employed in our work using the pulse oximetry is fast and generate results synchronously with all the processing done in parallel with the fingerprint identification module (in about 1.5 seconds). The spoof attacks from a very thin translucent fingerprint worn over a live finger generates low-quality fingerprint image from the employed optical sensor. Thus the rejection of such spoof attacks is also dependent on the quality-checker employed in the fingerprint identification module. Another kind of spoof attack that the liveness detection system may have to cope with involves attacker pulsing a pair of infrared and red LEDs underneath the spoof finger. However, in our system these external pulses cannot produce the variations in AC components introduced by the live tissue (pulse oximetry) through transmission. Assuming that even if this has been achieved by the attacker, the main problem would be the synchronization of these pulses with the excitation pulses of our system, which is not extremely difficult to achieve even if the attacker has the information about the frequency of the employed excitation pulses. There will always be a phase difference between the excitation and received signals, unless the attacker tampers the system and takes the excitation signal from our system to trigger his pulses. The excitation pulses of the LED indicators are generated by Pulse Width Modulation (PWM) and the ON/OFF time of the pulse is defined by two 16-bit registers respectively. Therefore, achieving correct synchronization with the excitation pulses is to find one point in a space of $2^{16} \times 2^{16}$ points. The analog to digital converter of the micro-controller is a 10-bit ADC, to spoof the system by externally generating an AC component would be of the order of 2^{10} . Therefore, to successfully spoof the system the attacker has to find one point in a space of $2^{16} \times 2^{16} \times 2^{10}$. Further, our

system takes 200 samples to calculate the SpO₂ value, as can be seen in figure 7 in the paper. This makes it a problem to find out one point in a space of $2^{16} \times 2^{16} \times 2^{12} \times 200 = 1$ in $8.796E+14$, which is certainly extremely difficult. The spectrographic characteristics of the live human tissue can also be used to ensure liveness using multispectral analysis of the finger [28]. However, the optical properties of gelatin artificial fingerprints are quite similar to human skin [30] and therefore such approaches are still prone to spoof attacks.

VII. CONCLUSIONS

A new anti-spoofing technique for fingerprint identification systems, using liveness detection has been proposed and implemented. This technique relies on the physiological behavior of the arterial blood volume and oxygen saturation level changes (principle of pulse oximetry). The oxygen saturation level of arterial blood (SpO₂%) is measured and used to ascertain the liveness decision from the presented biometric sample. The proposed liveness detection design has been integrated with the fingerprint device to develop a standalone liveness integrated fingerprint sensor. The proposed design and its standalone implementation using AT90USB1287 microcontroller has been rigorously tested.

In order to make the device standalone, and to integrate with the fingerprint sensor, an interfacing programming microcontroller based board, as shown in figure 5, was developed. The integration of this device with the fingerprint device is achieved by serial communication with this device and the decision of the fingerprint identification is being delivered to the host controller (AT90USB1287). The experimental results presented in section V, from several live and variety of non-live spoof fingerprint samples, have illustrated very high separation in the corresponding values of liveness factor R . The observed wide separation in the percentage of SpO₂ confirms the reliability of the proposed design to thwart spoof attacks on the fingerprint identification device. The developed device detects the liveness based on the SpO₂% and decides to integrate the fingerprint identification decisions from the live samples and deactivates the sensor for non-live samples. This device also displays the fingerprint identification status.

A summary of prior work on fingerprint antispoofing techniques, presented in section I A, has suggested that there has not been any systematic study to illustrate the effectiveness of oxygenated blood measurements in detecting spoofed fingerprints. Although more work remains to be done, this paper has successfully illustrated the utility of proposed low-cost and fully automated design that can simultaneously work with any fingerprint based identification device. Conclusively, the developed prototype of the liveness detection module, which is based on the estimation of the saturated oxygen level in the haemoglobin, has significantly higher anti-spoofing reliability as compared with several image or illumination based approaches, *e.g.* [11]-[12], presented in the literature. Our efforts are currently focused to further miniaturize the developed liveness detection module. It is

generally believed that any countermeasures to thwart biometric spoof attacks can be circumvented. The success of method investigated in this paper depends on the effectiveness of the fingerprint image quality checker employed in the fingerprint identification module. The antispoofting approach developed in this paper is tailored/limited to the optical fingerprint sensors that generate the image using the reflection of light from the finger valleys. Another possible method to circumvent this method is to develop spoof finger that can pulse a pair of infrared and red LEDs with a brute force attack, involving combinations of varying frequency and phase information. Therefore future efforts should be directed towards the large scale comparative evaluation of the effectiveness of various liveness detection approaches for such state-of-art sensor level spoof attacks.

VIII. ACKNOWLEDGMENT

This work is supported by the research grant from Department of Information Technology, Ministry of Information and Communication Technology, Government of India, grant no. 12(54)/2006-ESD.

REFERENCES

- [1] M. Drahansky, R. Notzel and W. Funk, "Liveness Detection based on Fine Movements of the Fingertip Surface", *Proc. IEEE Workshop on Information Assurance United States Military Academy*, West Point, pp. 42-47, NY, Jun. 2006.
- [2] A. B. Borreto, L. M. Vicente and I. K. Persad, "Adaptive Cancellation of Motion Artifact in Photoplethysmographic Blood Volume Pulse Measurements for Exercise Evaluation," *Proc. IEEE 17th Annual Conference on Engg. in Medicine and Biology Society*, vol. 2, pp. 983-984, 1995.
- [3] S. T. V. Parthasaradhi, R. Derakhshani, L. A. Hornak, and S. A. C. Schuckers, "Time-series detection of perspiration as a liveness test in fingerprint devices," *IEEE Trans. Systems Man, and Cybernetics, Part C*, vol.35, pp. 335 - 343, Aug. 2005.
- [4] N. K. Ratha, J. H. Connel, and R. M. Bolle, "Enhancing security and privacy in biometrics-based authentication systems," *IBM Syst. J.*, vol. 40, no. 3, pp. 614-634, 2001.
- [5] T. Matsumoto, H. Matsumoto, K. Yamada, and S. Hoshino, "Impact of Artificial Gummy Fingers on Fingerprint System", *Proc. SPIE*, vol. 4677, pp. 275-289, 2002.
- [6] Y. Shimada, K. Nakashima, Y. Fujiwara, T. Komatsu, M. Kawanishi, J. Takezawa and S. Takatani, "Evaluation of a new reflectance pulse oximeter for clinical applications," *J. of Med. & Biol. Eng & Comp.*, vol. 29, pp. 557-561, Sep. 1991.
- [7] H. Shimazu, H. Ito, and K. Yamakoshi, "Noninvasive method for estimating the mean capillary pressure and pre- and post capillary resistance ratio in human fingers," *Medical & Biological Engineering & Computing*, vol. 24, pp. 585-590, 1986.
- [8] T. Vander Putte and J. Keuning, "Biometrical fingerprint recognition: don't get your fingers burned", *Proc. 4th Working Conference of Smart Card Research and Advanced Applications*, pp. 289-303, Kluwer Academic, Sep. 2000.
- [9] Barbagelata, Melissa and H. Asada, "Wireless Fingernail Sensor for Continuous Long Term Health Monitoring", *MIT Home Automation and Healthcare Consortium Phase 3, Report 3-1*, Oct. 1, 2000.
- [10] http://www.atmel.com/dyn/resources/prod_documents/doc7593.pdf
- [11] K. Brownlee, Method and apparatus for distinguishing a human finger from a reproduction of fingerprint, *US Patent No. 6, 292, 571*, Sep. 2001.
- [12] D. R. Setlak, Fingerprint sensor having spoof reduction features and related methods, *US Patent No. 5, 953, 441*, Sep. 1999.
- [13] S.A.C. Schuckers, "Spoofing and Anti-spoofing measures," Information Security Technical Report, vol. 7, pp. 56-62, Dec. 2002.
- [14] U. Uludag and A.K. Jain, "Attacks on biometric systems: a case study in fingerprints," *Proc. SPIE-EI 2004, Security, Steganography and Watermarking of Multimedia Contents VI*, pp. 622-633, San Jose, CA, Jan. 18-22, 2004.
- [15] D. Osten, H. M. Carin, M. R. Arneson, and B. L. Blan, "Biometric Personal Authentication System," *U. S. Patent # 571, 9950*, Feb. 1998.
- [16] P. D. Lapsley, J. A. Less, D. F. Pare, and N. Hoffman, "Anti-fraud biometric sensor that accurately detects blood flow", *US Patent # 5,737,439*, April 7, 1998.
- [17] P. Kallo, I. Kiss, A. Podmaniczky, and J. Talosi, "Detector for recognizing the liveness character of a finger in fingerprint recognizing apparatus," *U. S. Patent # 6,175,641*, Jan. 2001.
- [18] V. Valencia and H. Horn, "Biometrics liveness testing," in *Biometrics*, J. D. Woodward, N. M. Orlans, and R. T. Higgins, Eds., New York: Osborne, McGraw Hill.
- [19] M. Drahanský, R. Nötzel, and W. Funk, "Liveness detection based on fine movements of the fingerprint surface," *Proc. 2006 IEEE workshop on Information Assurance*, United States Military Academy, New York, pp. 42-47, 2006.
- [20] J. Kent, Malaysia car thieves steal finger, BBC News, Kuala Lumpur, <http://news.bbc.co.uk/2/hi/asia-pacific/4396831.stm>
- [21] A. Antonelli, R. Capelli, D. Maio, and D. Maltoni, "Fake finger detection by skin distortion analysis," *IEEE Trans. Info. Forensics & Security*, vol. 1, pp. 360-373, Sep. 2006.
- [22] Y. S. Moon, J. S. Chen, K. C. Chan, K. So, and K. C. Woo, "Wavelet based liveness detection," *Electronics Letters*, vol. 41, pp. 1112-1113, Sep. 2005.
- [23] A. Adler, "Sample images can be independently restored from the face recognition templates," *Proc. Canadian Conf. Electrical Computer Engg. (CCECE)*, Montréal, Canada, pp. 1163-1166, May 2003.
- [24] B. Toth, "Biometric liveness detection," *Information Security Bulletin*, vol. 10, pp. 291-297, Oct. 2005.
- [25] A. Abhyankar and S. Schuckers, "Fingerprint liveness detection using local ridge frequencies and multi resolution texture analysis techniques," *Proc. ICIP 2006*, pp. 321-324, Oct. 2006.
- [26] S. A. Wilber, "Blood constituent measuring device and methods," *U. S. Patent # 4,407,290*, Apr. 1983.
- [27] R. T. Stone and D. A. Briggs, "Method and apparatus for calculating oxygen saturation based plethysmographs including transients," *U. S. Patent # 5,078,136*, Jul. 1992.
- [28] K. A. Nixon, R. K. Rowe, J. Allen, S. Corcoran, L. Fang, D. Gabel, D. Gonzales, R. Harbour, S. Love, R. McCaskill, B. Ostrom, D. Sidlauskas, and K. Unruh, "Novel spectroscopy-based technology for biometric and liveness verification," *Proc. SPIE*, vol. 5404-27, pp. 287-295, Aug. 2004.
- [29] G. Zonios, U. Shankar, and V. K. Iyer, "Pulse oximetry theory and calibration for low saturations," *IEEE Trans. Biomedical Engineering*, vol. 51, pp. 818-822, May 2004.
- [30] D. Maltoni, D. Maio, A. K. Jain, and S. Prabhakar, *Handbook of Fingerprint Recognition*, Springer Verlag, 2003.
- [31] P. E. Philip, J. R. Feiner, and J. W. Severinghaus, "Effects of skin pigmentation on pulse oximeter accuracy at low saturation," *Anesthesiology*, vol. 102, no. 4, pp. 715-719, 2005
- [32] N. K. Ratha, J. H. Connell, and R. M. Bolle, "Enhancing security and privacy in biometrics-based authentication systems," *IBM Systems Journal*, vol. 40, no. 3, pp. 614-634, 2001.
- [33] J. W. Severinghaus and S. O. Koh, "Effect of anemia on pulse oximeter accuracy at low saturation," *J. Clinical Monitoring & Computing*, vol. 6, no. 2, April 1990.